A three-dimensional dual-mechanism model of pore stability in a sintering alumina structure

Darcovich, Kenneth; Shinagawa, K.; Walkowiak, F.

Publisher's version / Version de l'éditeur:
https://doi.org/10.1016/j.msea.2003.12.037
Materials Science and Engineering A, 373, 2004

Materials Science and Engineering A 373 (2004) 107–114

www.elsevier.com/locate/msea

A three-dimensional dual-mechanism model of pore stability in a sintering alumina structure☆

K. Darcovich[a,*], K. Shinagawa[b], F. Walkowiak[c]

[a] National Research Council of Canada, Institute for Chemical Process and Environmental Technology, Ottawa, Ont., Canada K1A 0R6
[b] Department of Advanced Materials Science, Faculty of Engineering, Kagawa University, Hayashi-cho 2217-20, Takamatsu 761-0396, Japan
[c] ICAM-Toulouse, 75, av. de Grande Bretagne, Toulouse 31300, France

Received 7 July 2003; received in revised form 22 December 2003

Abstract

A three-dimensional simulation based on a cubic configuration of sintering grains was formulated to study the evolution of pore morphology. A numerical simulation treating lattice diffusion derived from a viscoplastic formulation was used as the basis for the work. The additional mechanism of surface diffusion was incorporated into the simulation. An objective in a broader context is to design nano-scale filtration media. At this size scale, tracing the evolving pore morphology with any degree of accuracy in three dimensions requires the simultaneous application of relevant sintering mechanisms. The paper details the formulation of the model and presents a quantitative comparison to some benchmark experimental data. An example result demonstrates that the coded model was able to simulate the pore morphology evolution in a plausible manner. At length scales below 10^{-6} m, significant morphological differences are observed for simultaneous surface and lattice diffusion compared to considering only lattice diffusion.

Keywords: Simultaneous surface and lattice diffusion mechanisms; Sintering; Pore evolution; Three-dimensional; Alumina

1. Introduction

In order to process ceramic powder into materials suitable to function as filtration membranes, a certain amount of sintering is required to bond the powder compact into a strong and contiguous structure. For specific filtration needs such as gas separations, a near exact pore size is required to achieve the desired separation of two closely sized species.

Often in pressureless sintering of metals and ceramics, the materials exhibit viscoplastic flow. Many researchers have studied the deformation behavior of viscous porous materials at elevated temperatures. Coble [1] developed a model for bulk or lattice diffusion based on geometrical structure and contact surfaces. This model was then extended [2] to account for a creep rate in polycrystalline materials, thus able to account for the coalescence and densification occurring between neighboring grains under the lattice diffusion mechanism.

This subject was advanced in a paper by Svoboda and Reidel [3] where the lattice diffusion model was adapted to real neck geometries determined by accounting for surface energy minimization criteria. Using similar energy considerations, Parhami et al. [4] simulated a linear row of sintering particles incorporating coarsening effects where unequal sized particles were involved.

The above work has lead to the present model first shown by Shinagawa [5] which made use of a surface energy boundary condition to trace the evolution of a pore inside a cubic grain arrangement, and later further studied [6] to relate the micro-level model to larger structures.

In the present case, where sintering is to be considered from initial, right through until late stages, the simultaneous treatment of sintering mechanisms is important. Surface diffusion is a key mechanism which will have significant impact on the evolution of an inter-grain pore. It is therefore the objective of the present paper to expand the mircomechanical sintering model developed by Shinagawa [6] that was originally formulated with only lattice diffusion as a sintering mechanism. Surface diffusion, especially important in initial stages of sintering, is an essential mechanism to incorporate into the simulation to more correctly model

☆ NRCC No. 46460.

* Corresponding author. Tel.: +1-613-993-6848; fax: +1-613-941-2529.
E-mail address: ken.darcovich@nrc-cnrc.gc.ca (K. Darcovich).

0921-5093/$ – see front matter © 2004 Elsevier B.V. All rights reserved.
doi:10.1016/j.msea.2003.12.037

the neck formation at particle interfaces and subsequent pore evolution.

2. Finite element analysis of the sintering process in an open pore structure

2.1. Basic microscopic model—lattice diffusion

The particles in real powder compacts are arranged randomly and the powder compacts can be regarded as a body having pores with various complex shapes. In the present study, a repeating unit cell with a regular pore arrangement is employed since it is a manageable geometry. The model of an open pore surrounded by particles in a cubic arrangement is shown in Fig. 1. The finite element mesh used in this analysis is also depicted in Fig. 1. Due to the symmetry of the geometry and the deformation, only one-eighth part of the unit cell is treated.

The sintering process must be simulated with a number of constants, initial properties and boundary conditions. On the surface plane of symmetry for the unit cell, the tangential components of the nodal velocities are taken to be zero. To keep the continuity of the unit cell, the normal components of the nodal velocities on the cell boundary are constrained to be equal. The initial neck radius is taken to be 0.01 times the particle radius. This allows the surface diffusion and grain-boundary mechanisms to operate and simulate the initial stages of sintering where the neck regions are formed before any significant shrinking occurs. The stepwise calculation in the finite element scheme is carried out until the open pore reaches 0.34 nm, which is a desired dimension for the separation of CO_2 from N_2.

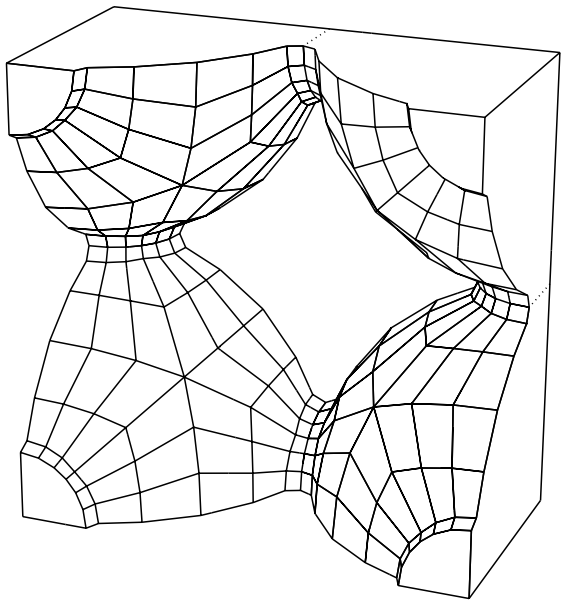

Fig. 1. Geometrical representation of the physical domain treated by the finite element sintering simulation.

The basic mechanism first incorporated into the model was lattice diffusion which accounts for some grain deformation and was treated by a viscoplastic model adapted for polycrystalline materials such as alumina, considered here. Details of the formulation for this mechanism are given by Shinagawa [6]. Its basis is a viscous creep expression developed by Coble [2], which relates the stresses arising in sintering σ to a strain rate $\dot{\bar{\varepsilon}}$, and,

$$\bar{\sigma} = 3\eta\dot{\bar{\varepsilon}} \tag{1}$$

where η is known as a viscosity term for this deformation process. Eq. (1) is cast into a matrix form and manipulated to relate nodal forces in an FEM grid to the consequent displacements. The nodal forces are equilibrated by being set to zero at internal points in the grains, and to a traction arising from the geometry and surface tension on the pore surface. The formulation detailed in [6] is the same as that used in the present work for the lattice diffusion mechanism.

2.2. Material properties

The material considered for simulation here were spherical alumina particles of 200 nm diameter. Relevant material properties required to calculate diffusion rates are given in Table 1 [7,8]. The diffusion expressions are based on a temperature dependent expression of the form,

$$D_{\mathrm{m}} = D_{\mathrm{m0}} \exp\left(-\frac{Q_{\mathrm{m}}}{RT}\right)$$

where Q is the activation energy, R the gas constant, T the temperature in Kelvin and the subscript m refers to the diffusion mechanism being considered. In the present work, grain boundary diffusion constants are used with the subscript b, and surface diffusion constants use the subscript s.

With deformation modeled by viscous flow, grain boundary diffusion coefficients can be used since the underlying mechanism is the same, only the diffusional paths change. To accommodate this, Coble's expression used for the deformation viscosity [6] is modified by using the grain diameter to the third power rather than the second. In this sense the change in the diffusion paths affects only the magnitude of the viscosity.

Table 1
Physical constants for alumina used in the simulations

Parameter	Value	Units
D_{s0}	4.8×10^{-9}	m^2/s
Q_{s}	4.34×10^{5}	J/mol
D_{b0}	1.23×10^{-9}	m^3/s
Q_{b}	4.39×10^{5}	J/mol
Ω	4.254×10^{-29}	m^3
γ	$1.117 + 1.0 \times 10^{-4}T$	N/m

2.3. Surface diffusion mechanism

When considering particles of diameters below 1 μm, it is important and necessary to incorporate the effects of surface diffusion into a simulation treating the various stages of sintering. Surface diffusion is an important mechanism contributing to neck formation, since it is driven by curvature differences, which are quite pronounced in the early stages. In a sense, the extent of curvature dictates the relative frequency of lattice defects which allow ionic diffusion in the surface layers.

The basic equation governing material flux due to surface diffusion is as follows,

$$J_s = \frac{D_s \Omega \gamma}{kT} \frac{\partial K}{\partial S} \tag{2}$$

where D_s is the surface diffusion coefficient, Ω the atomic volume of the diffusing species, γ the interfacial tension between the ceramic surface and air, k the Boltzmann's constant, T the temperature and $\partial K/\partial S$ term represents the local curvature gradient. A volumetric flux can be determined from Eq. (2) by considering a local element of volume.

$$\frac{dV}{dt} = J_s \delta_s w \tag{3}$$

where δ_s is a surface thickness in which the surface diffusion mechanism operates, and w is a cell width as applied to the finite element method. The value for δ_s was taken to be three molecular diameters.

2.4. Numerical treatment of surface diffusion

The present advance involved correctly implementing the surface diffusion equation into the pre-existing code treating the lattice diffusion. Numerically, the most difficult and sensitive term to express in the calculations was the surface curvature, and in particular, evaluating the $\partial K/\partial S$ term on irregular 3D gridded points, which formed the geometrical basis of our simulation.

Surface diffusion is a process that transfers matter to local regions of high curvature such as the particle neck. The process reaches equilibrium when a surface becomes uniformly curved. From the symmetry in a cubic configuration there are no differences of curvature in the planes parallel to the neck plane. In view of this, it was only necessary to treat the surface diffusion in the radial direction.

Through symmetry, the problem could be treated in a single dimension. Working only with the grid points along one radial line would not provide sufficient numerical resolution needed to obtain quantitatively or even qualitatively correct sintering behavior. However these points could be used as the basis for a high-resolution spline which was mathematically quite smooth.

To begin the process, the one-dimensional section to be treated could be restricted to a curve extending in a direction normal to the neck face, as depicted in Fig. 2. Curves

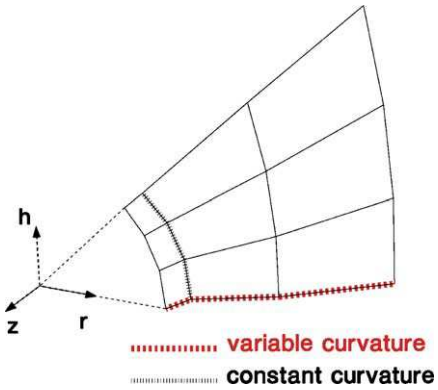

Fig. 2. Portion of domain required for surface diffusion calculation. Calculations over the rest of the assembly can be made through symmetry.

which are parallel to the neck face have a curvature gradient of zero and thus there are no contributions to surface diffusion in this direction. A line on the plane $h = 0$ was selected for this procedure, to involve only two cartesian dimensions in the surface diffusion calculation. Deformations on other parts of the three-dimensional grain would be determined by a mapping of these rz-plane results. For the lattice diffusion mechanism operating throughout the grain volume, a domain consisting of 427 nodes was constructed. Through symmetry, only nine surface faces (as depicted in Fig. 2) need be considered.

Again, through symmetry, node points outside of the range requiring treatment are appended in external regions (points 1, 6 and 7 in Fig. 3), either on the main part of the grain or on the neck region of a neighboring grain. These points, P_i are used as a preliminary basis for spline-fitting the surface curve. The space curve coordinate s is calculated and stored from a line integral along surface. Components of the unit normal $\vec{\mathbf{n}}$, n_z and n_r are calculated based on the local slopes defined by neighboring points.

Since the spline nodes themselves can contain discontinuities for curvature calculations (i.e., the second derivatives may not be smooth functions over break points) a series of intermediate points was selected as indicated as ${}_2P_i$ in Fig. 3.

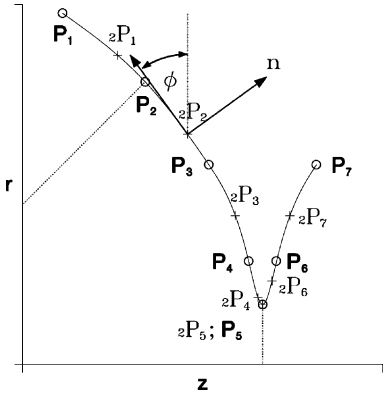

Fig. 3. Initial discretization of surface contour of grain on plane $h = 0$ for surface diffusion simulation.

At the ${}_2\mathrm{P}_i$ points, some parameters required for the fundamental equations (Eqs. (2) and (3)) are calculated. An angle ϕ (depicted in Fig. 3) which is relevant to curvature calculations was also calculated locally with the ${}_2\mathrm{P}_i$ spline. Considering the surface in spherical coordinates, the two principal radii of curvature, K_a and K_b can be calculated from ϕ as [9],

$$K_a = \frac{\mathrm{d}\phi}{\mathrm{d}s} \tag{4}$$

$$K_b = \frac{-\sin\phi}{r} \tag{5}$$

A second spline function of $\phi(s)$ based on the ${}_2\mathrm{P}_i$ points is then calculated. Values for the angle ϕ from this second spline are subsequently evaluated at the nodes determined from the P_i curve to get K_a and K_b. If K_a and K_b are determined directly from the spline based on the P_i points, the behavior in the simulation was found to be unreliable, owing to instabilities arising at positions near the original grid points.

Reexpressing Eq. (2) in a discretized form gives,

$$j_i = \frac{D_\mathrm{s}\Omega\gamma}{kT}\left(\frac{K_{i+1}-K_{i-1}}{s_{i+1}-s_{i-1}}\right) \tag{6}$$

For the first and last points along the curve, the above expression is modified to consider only the end point and its neighbor on the curve. Now for an element along the line, the net volume change arising from surface diffusion will be the sum of the exchanges between its two neighbors. That is,

$$V_i = \left[\frac{r_i + r_{i-1}}{2} j_i - \frac{r_{i+1}+r_i}{2} j_{i+1}\right]\Delta t \tag{7}$$

For the last point on the curve (i.e., P_5 in Fig. 3, the mid-point of the neck surface contour) the expression for V_i through symmetry becomes simply two times the first term of Eq. (7). This condition implies a 180°dihedral angle. Knowing the volume changes over each element now allows us to calculate the displacement of the points on the surface. The mid-points between nodes are employed to define where the volume changes apply. Fig. 4 depicts a schematic of the parameters used in calculating the surface displacements caused by local volume transfers. The volume transferred into or out of this cell is known from the diffusion relations. Geometrically, we model the change as a build-up or removal of material over the surface of the element in a direction normal to where the central node is located. This is shown by the vector n in Fig. 4 at the point (z_i, r_i). The displacement of the node will be a total distance indicated as $\mathrm{d}\ell$ which can be determined explicitly through the following equation, based on a volume of revolution around the z-axis.

$$V_i = \int_{z_\mathrm{BL}}^{z_\mathrm{TL}} (f_\mathrm{L}^2 - f_\mathrm{B}^2)\,\mathrm{d}z + \int_{z_\mathrm{TL}}^{z_\mathrm{BR}} (f_\mathrm{T}^2 - f_\mathrm{B}^2)\,\mathrm{d}z + \int_{z_\mathrm{BR}}^{z_\mathrm{TR}} (f_\mathrm{T}^2 - f_\mathrm{R}^2)\,\mathrm{d}z \tag{8}$$

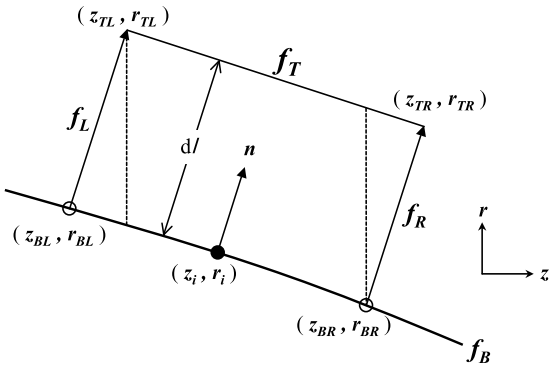

Fig. 4. Schematic for the calculation of the surface displacement $\mathrm{d}\ell$ from surface diffusion. The indices L, B, R and T refer, respectively, to the left, bottom, right and top surfaces of the volume of revolution. The terms f_j refer to function expressions for the four surfaces.

Finally, to end an iteration, the displacements were applied to the node positions to calculate the new surface at the end of the time step. This was done according to,

$$r_{i\,\mathrm{NEW}} = r_i + n_r\,\mathrm{d}\ell \tag{9}$$

$$z_{i\,\mathrm{NEW}} = z_i + n_z\mathrm{d}\ell \tag{10}$$

2.5. Algorithm for simultaneous simulation of mechanisms

Numerically, it was found that the lattice diffusion simulation on its own was far more stable over time steps than the surface diffusion simulation. Consequently, careful treatment was required for the two different time step controls in order to have them properly simulating simultaneous effects in sintering grains.

In the initial stages, changes brought about by the surface diffusion mechanism were more dramatic, and thus required very small time steps so that high diffusion rates based on beginning conditions did not translate into physically unrealistic geometries. For the case under consideration, which was alumina grains of 200 nm diameter being sintered at 1300 °C, time steps of up to 60 s produced similar and stable results for the lattice diffusion mechanism. It was found that numerical stability for the surface diffusion mechanism required time steps about 1000 times smaller than that of the lattice diffusion mechanism. This was investigated by checking the details of the surface profiles generated by single time steps. In principle, a surface should not be transformed over a time step such that it violates the driving force of the mechanism which seeks an increasingly uniform degree of curvature on the surface in question. Too long a time step can result in local bumps forming on the surface, which are physically unrealistic and appear only as a numerical artefact from the simulation parameters. Fig. 5 illustrates this situation. The main concept is that the diffusion rate is calculated based on the original geometry, and the ensuing mass transfer is implemented with the time step as a multiplier. If the time step is too long, it implies that that kinetic rates are in

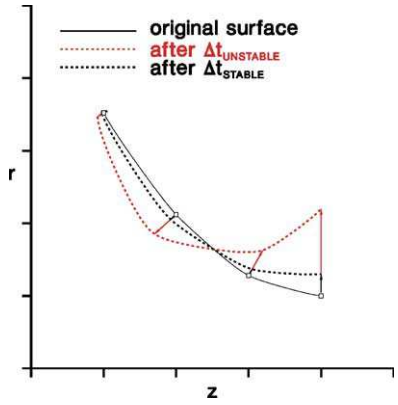

Fig. 5. Schematic showing implied physical effect of too large a time step creating an implausible neck surface.

effect long after the geometry that gave rise to them no longer exists in the same way. The normal vectors in Fig. 5 show the directions and relative proportions in which the mass transfer will move points, as the $d\ell$ term is a function of the diffusion rate. The extent of the change is governed by the time step. If the time step is too long in the numerical simulation, a non-plausible or unstable geometry will result. Numerical checks were implemented in the code to control time step sizes, both to shrink or expand them to maximize computational efficiency. Control of the time step for the surface diffusion mechanism was one of the key challenges in making a properly functioning two-mechanism sintering code.

Additionally, at some particular positions, such as the mid-point of the neck surface, it is known that the slope must be zero, so any time step chosen which is too large will produce an r coordinate for the end point greater than its neighbor, clearly in error. In terms of the sintering process, what this means is that the driving forces change substantially, even over this short of a time step, so that applying the calculated diffusion rate over a reduced time step would more accurately reflect the kinetics of the process. As suggested by Fig. 5, the displacements during a time step must be much less than the positional differences of the nodes in the r-direction at the start of the iteration.

3. Project scope

The scope of the present study entails developing and implementing a surface diffusion model for sintering to be implemented on the three-dimensional system of an evolving pore created inside eight spherical grains arranged cubically. In order to verify that the routine is operating properly, the surface diffusion mechanism could be run independently. Although this is not physically realistic, obtaining an equilibrium structure with uniform surface curvature would be the necessary outcome. Further, the kinetics of this evolution could be verified against theoretical predictions for neck growth during the early stages of sintering.

With a satisfactory algorithm for the surface diffusion mechanism, the simulation then will be run for cases with only lattice diffusion and another with simultaneous surface and lattice diffusion. These tests are intended to demonstrate the key differences between these two cases, providing a basis to comment on what ramifications these results entail for pore evolution modeling.

4. Results and discussion

4.1. Surface diffusion mechanism

Validation of the surface diffusion algorithm was done through two checks, one for rate and one for morphology. To verify the plausibility of the kinetics of the simulation the rate of neck growth in the early stages of sintering was investigated. There exist some classical models which make predictions for the rate of neck growth as a fraction of grain diameter (x/a) for various diffusion mechanisms. Here, x is the diameter of the narrowest part of the neck, and a is the original grain diameter. The simulation by Bouvard and McMeeking [9] was verified against the theoretical model presented by Coblenz et al. [10] whose expression for early stage neck growth is,

$$\frac{x}{a} = \left(\frac{225t}{\tau_s}\right)^{1/5} \tag{11}$$

Above, τ_s is a characteristic time given by,

$$\tau_s = \frac{kTR^4}{\delta_s D_s \Omega^2 \gamma}$$

where $R = a/2$.

Fig. 6 shows a plot of x/a versus the dimensionless sintering time for the present simulation. A grain of unit radius was considered. Also shown are data from the Bouvard simulation and the Coblenz theoretical model. Up until an x/a ratio of about 0.08, the three estimates are fairly similar. For $x/a > 0.10$, the present simulation shows a more rapid rate of neck growth. A main reason for these differences is that the Coblenz and Bouvard estimates were based on two-grain systems, and the present work considers a cubic arrangement of spheres. At the very early stages, the material arriving in the neck region is local, so the rates ought to be similar. As the process continues however, a two-sphere system will attain more overall uniformity of curvature than the cubic arrangement, so the growth rate decelerates. Also, material has to travel from all regions of two spheres, while in a cubic arrangement, the material arriving at a neck is all from the nearest one-sixth of each of the two contributing grains. The lack of smoothness in the curve showing the present simulation in Fig. 6 can be attributed to the relative coarseness of the mesh. Although a 1500 point spline was used to drive the surface diffusion, the grains were constructed in three dimensions in a mesh containing 427 nodes.

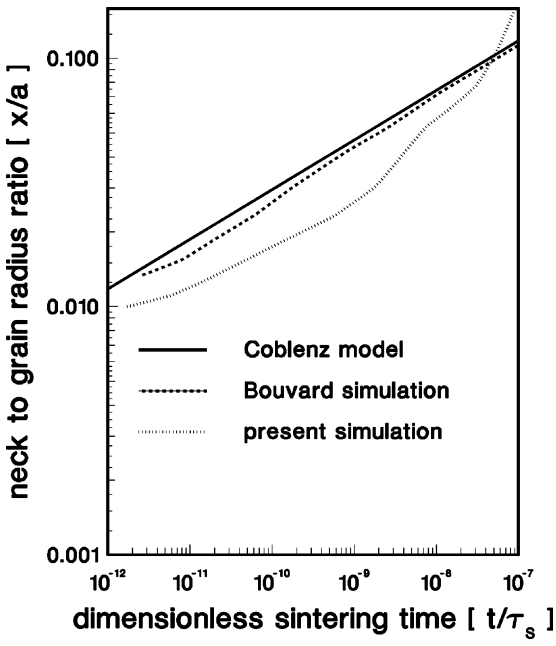

Fig. 6. A comparison of the present simulation against a classical model and a simulation by Bouvard and McMeeking [9] for x/a vs. dimensionless time.

To validate the structures predicted by the surface diffusion mechanism modeled in the present simulation, the simulation was allowed to run for a very large number of time steps where the shape attained was an equilibrium surface with uniform surface curvature everywhere in the structure. Fig. 7 shows the evolving structure produced by a cubic arrangement of grains under the theoretical conditions of pure surface diffusion. A time step of $t = 2.0 \times 10^{26}$ s was used producing a dimensionless time step of $t/\tau_s = 1.7 \times 10^{-12}$. Such a seemingly huge time step is required because a unit radius implies a grain of 1 m in diameter with MKS units.

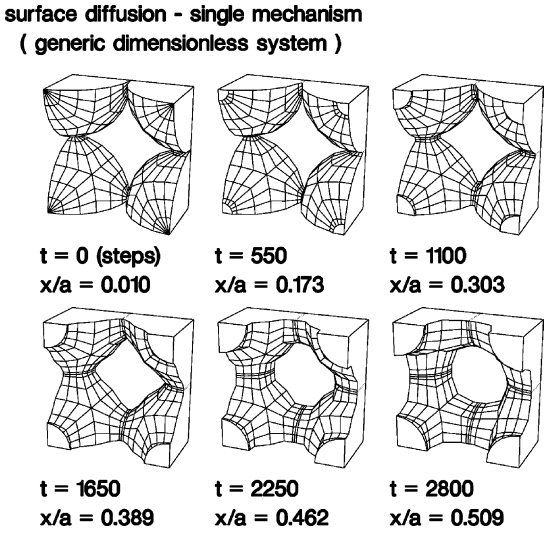

Fig. 7. Pore evolution simulated using only the surface diffusion mechanism with dimensionless parameters.

After the first 100 iterations, the time step was increased to $t/\tau_s = 5.0 \times 10^{-10}$. After 2800 time steps, the simulation showed the structure in the bottom right of Fig. 7. The simulation was continued to 4000 time steps, and the structure remained unchanged. Checks of surface curvature on the structure revealed a variance of less than 1%. The structure in Fig. 7 matches a diagram of an equilibrium calculation performed by Svoboda et al. [11] for a 180°dihedral angle.

The displacement calculated in Eq. (8) is an improvement on the method employed by Bouvard and McMeeking [9], which was based on a ring volume calculated in a plane normal to the rz-plane. This was verified when the sum of the volume changes over all the elements was determined. For every iteration, the extent of discrepancy and need for adjustment was about 1–2% of that required by Bouvard et al.'s method. A uniform fractional adjustment was applied to all the $d\ell$ values calculated along the surface to conserve the original volume. For a discretization of the line into about 1500 points, the original Bouvard method usually generated a $\Delta V/V_{ORIG.} \approx 10^{-3}$, while this value was closer to 10^{-5} using Eq. (8).

Thus, the results presented in Figs. 6 and 7 suggest that the surface diffusion mechanism was correctly coded and implemented. These tests provide justification for moving forward with the surface diffusion mechanism and combining it with the lattice diffusion mechanism to examine simultaneous effects.

4.2. Combined lattice and surface diffusion

The lattice diffusion mechanism was previously formulated and demonstrated in a numerical simulation by Shinagwawa [6]. In that work, the model compared favorably with data presented by Coble [1] for the sintering of alumina. For the alumina particles considered here, the morphological evolution for sintering with simultaneous surface and lattice diffusion at 1300 °C is shown in Fig. 8. The sintering was allowed to proceed up until the pore diameter decreased to 0.34 nm, a dimension related to the sieving of combustion gases. The process took 72 min, which compares plausibly with data for larger 300 nm alumina [1,6] with a larger starting neck size. Data from Lim et al. [12] for 180 nm diameter alumina shows about 96% theoretical density for 1 h of sintering at 1300 °C. The densification rates match well given that the grains from the Lim et al. experiments were slightly smaller, and the entire suite of 5 or so simultaneous mechanisms would be taking place with real particles.

It is instructive to compare the results shown in Fig. 8 with those in Fig. 9 obtained under the same initial conditions and with the same processing parameters, but with only the lattice diffusion mechanism active. It can be seen that over the same 72 min period, the difference in theoretical density achieved is about 0.10. The surface diffusion mechanism serves to increase the neck size right from the early stages of sintering. This then allows the lattice diffusion mechanism to operate over a larger transfer region and accelerate the

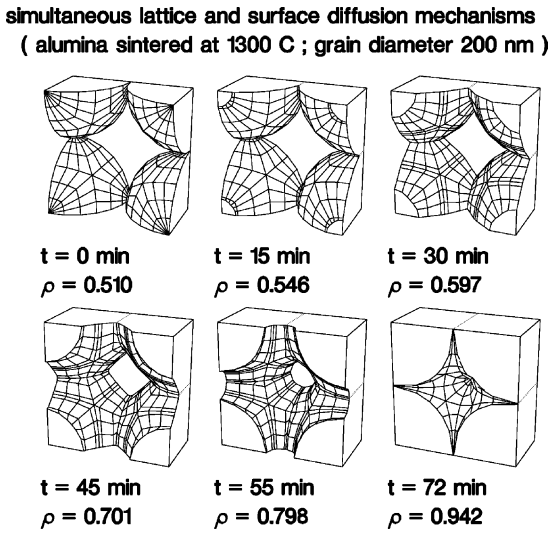

Fig. 8. Pore evolution simulated with simultaneous surface and lattice diffusion mechanisms for 200 nm diameter alumina sintered at 1300 °C.

densification. The morphology itself is similar up to around 30 min of sintering. Beyond 30 min, it is visible in Fig. 8 that the surface and pore contours are more rounded and that the pore size itself is noticeably smaller. Fig. 10 shows a plot of the neck size versus sintering time for the two cases. Here the early stages of sintering produce neck growth at a higher rate which produces a difference which carries over for the rest of the process. Correspondingly Fig. 11 shows density versus time for the two cases. The density begins to increase at a visibly higher rate beyond 30 min, which can be attributed to a larger interparticle transfer area created by the inclusion of the surface diffusion mechanism.

Finally, the pore shrinkage can be examined. The pore size is reduced at very similar rates for the dual-mechanism simulation compared to lattice diffusion only, for much of

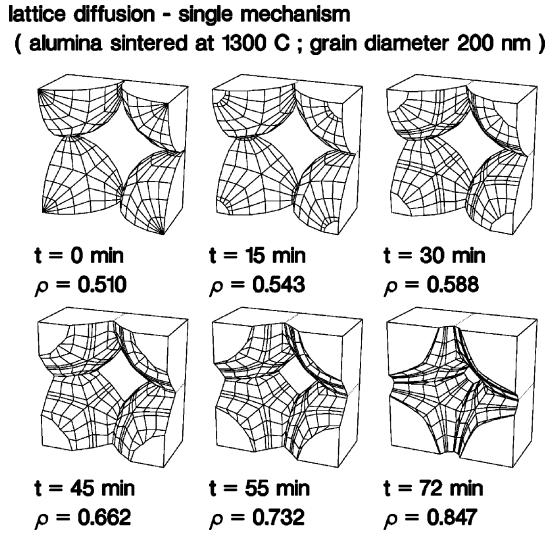

Fig. 9. Pore evolution simulated using only the lattice diffusion mechanism for 200 nm diameter alumina sintered at 1300 °C.

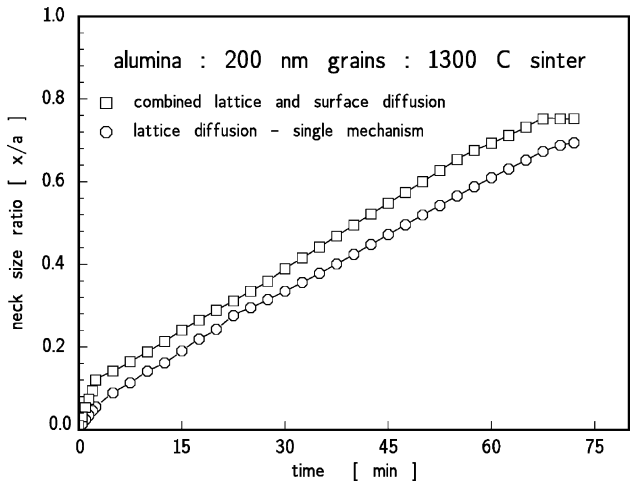

Fig. 10. Neck size vs. time for 200 nm diameter alumina sintered at 1300 °C.

the sintering time. Slight differences in neck size may only produce small differences in the calculated pore dimensions since there is only a very small volume of material accumulated in the neck regions, and the pore dimension itself is essentially a bulk property. In the later stages of the process however, the size of the pore becomes so small that the curvature along its face becomes high enough to become a material sink for the surface diffusion mechanism. Further as the dimension of the pore approaches zero, any contribution of material onto its surface will apparently accelerate the reduction of the pore diameter. This shows up more explicitly on a log-scale in Fig. 12, where the pore diameter is plotted against the sintering time.

Modeling of pore closure was not attempted in this project. As such, all states shown in Figs. 8 and 12 represent open pores. Presumably, if this simulation was continued beyond $t = 72$ min, when the amount of diffusion to the pore surface in one time step exceeds the volume available, the pore would be considered closed and curvature

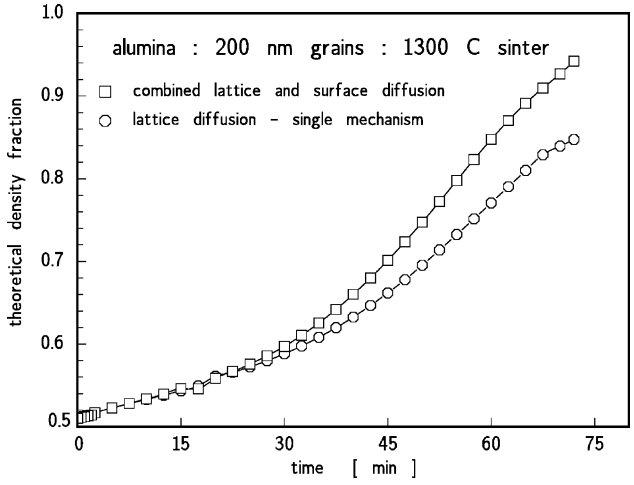

Fig. 11. Density vs. time for 200 nm diameter alumina sintered at 1300 °C.

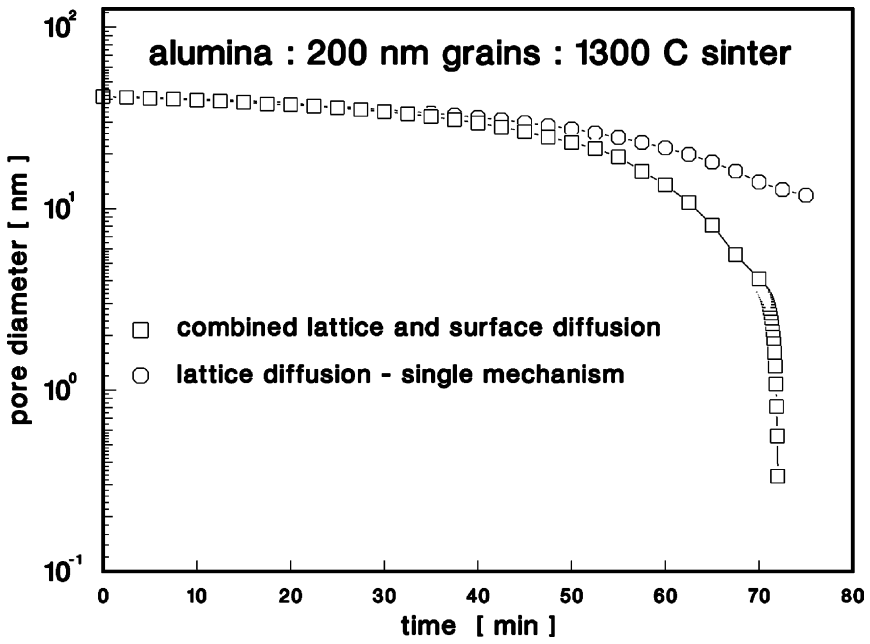

Fig. 12. Pore diameter vs. time for 200 nm alumina sintered at 1300 °C.

differences in all three dimensions could be considered to continue tracing the internal morphology of a closed-pore structure. This is an interesting problem for future research.

5. Conclusions

This project successfully demonstrated the development and implementation of a three-dimensional simulation for the surface diffusion mechanism of sintering of alumina particles positioned in a cubically packed structure. Through verification of both kinetic and morphological outcomes, it can be confidently stated that the surface diffusion sintering routine simulated correctly. When combined with a pre-existing lattice diffusion routine, the evolution of a cubically packed structure of 200 nm diameter alumina grains sintered at 1300 °C showed significant differences under the dual-mechanism mode compared to implementing only lattice diffusion. For sub-micron sized particles, the surface diffusion mechanism is essential for the study of pore morphology since the neck growth in early stages of sintering and the pore closure at the late stages of sintering were shown to proceed at significantly different rates in the dual-mechanism mode.

References

[1] R.L. Coble, J. Appl. Phys. 32 (5) (1961) 787.
[2] R.L. Coble, J. Appl. Phys. 34 (6) (1963) 1679.
[3] J. Svoboda, H. Riedel, Acta Metall. Mater. 40 (11) (1992) 2829.
[4] F. Parhami, R.M. McMeeking, A.C.F. Cocks, Z. Suo, Mech. Mater. 31 (1) (1999) 43.
[5] K. Shinagawa, JSME Int. J. Ser. A 39 (4) (1996) 565.
[6] K. Shinagawa, Comp. Mater. Sci. 13 (1999) 276.
[7] E. Dörre, H. Hübner, Alumina, Springer-Verlag, Berlin, 1984.
[8] R.M. Cannon, W.H. Rhodes, A.H. Heuer, J. Am. Ceram. Soc. 63 (1–2) (1980) 46.
[9] D. Bouvard, R.M. McMeeking, J. Am. Ceram. Soc. 79 (3) (1996) 666–672.
[10] W.S. Coblenz, J.M. Dynys, R.M. Cannon, R.L. Coble, in: G.C. Kuczynski (Ed.), Proceedings of the Fifth International Conference on Sintering and Related Phenomena, Plenum Press, New York, 1980, p. 41.
[11] J. Svoboda, H. Riedel, H. Zipse, Acta Metall. Mater. 42 (2) (1994) 435.
[12] L.C. Lim, P.M. Wong, J. Ma, J. Mater. Process. Technol. 67 (1997) 137.